NUMERICAL SOLUTION OF AN INTEGRO-DIFFERENTIAL EQUATION ARISING IN OSCILLATING MAGNETIC FIELDS

KOUROSH PARAND[1,2,†] AND MEHDI DELKHOSH[1]

[1] DEPARTMENT OF COMPUTER SCIENCES, SHAHID BEHESHTI UNIVERSITY, TEHRAN, IRAN.
E-mail address: k_parand@sbu.ac.ir
E-mail address: mehdidelkhosh@yahoo.com

[2] DEPARTMENT OF COGNITIVE MODELLING, INSTITUTE FOR COGNITIVE AND BRAIN SCIENCES, SHAHID BEHESHTI UNIVERSITY, TEHRAN, IRAN.

ABSTRACT. In this paper, an integro-differential equation which arises in oscillating magnetic fields is studied. The generalized fractional order Chebyshev orthogonal functions (GFCF) collocation method used for solving this integral equation. The GFCF collocation method can be used in applied physics, applied mathematics, and engineering applications. The results of applying this procedure to the integro-differential equation with time-periodic coefficients show the high accuracy, simplicity, and efficiency of this method. The present method is converging and the error decreases with increasing collocation points.

1. INTRODUCTION

In this section, Spectral methods and some basic definitions and theorems which are useful for our method have been introduced.

1.1. **Spectral methods.** Spectral methods have been developed rapidly in the past two decades. They have been successfully applied to numerical simulations in many fields, such as heat conduction, fluid dynamics, quantum mechanics, etc. These methods are powerful tools to solve differential equations. The key components of their formulation are the trial functions and the test functions. The trial functions, which are the linear combinations of suitable trial basis functions, are used to provide an approximate representation of the solution. The test functions are used to ensure that the differential equation and perhaps some boundary conditions are satisfied as closely as possible by the truncated series expansion. This is achieved by minimizing the residual function that is produced by using the truncated expansion instead of the exact solution with respect to a suitable norm [1, 2, 3, 4, 5, 6, 7, 8, 9, 10].

1.2. **Basical definitions.** In this section, some basic definitions and theorems which are useful for our method have been introduced [11].

Definition 1. For any real function $f(t)$, $t > 0$, if there exists a real number $p > \mu$, such that $f(t) = t^p f_1(t)$, where $f_1(t) \in C(0, \infty)$, is said to be in space C_μ, $\mu \in \Re$, and it is in the space C_μ^n if and only if $f^n \in C_\mu$, $n \in N$.

Definition 2. The fractional derivative of $f(t)$ in the Caputo sense by the Riemann-Liouville fractional integral operator of order $\alpha > 0$ is defined as [12, 13]:

$$D^\alpha f(t) = \frac{1}{\Gamma(m-\alpha)} \int_0^t (t-s)^{m-\alpha-1} D^m f(s)\, ds, \ \alpha > 0,$$

for $m - 1 < \alpha \leq m$, $m \in N$, $t > 0$, m is the smallest integer greater than α, and $f \in C_{-1}^m$. Some properties of the operator D^α are as follows. For $f \in C_\mu$, $\mu \geq -1$, $\alpha, \beta \geq 0$, $\gamma \geq -1$, $N_0 = \{0, 1, 2, \cdots\}$ and constant C:

$$(i) \quad D^\alpha C = 0,$$

$$(ii) \ \ D^\alpha D^\beta f(t) = D^{\alpha+\beta} f(t), \tag{1.1}$$

$$(iii)\ D^\alpha t^\gamma = \begin{cases} 0, & \gamma \in N_0 \text{ and } \gamma < \lceil \alpha \rceil, \\ \\ \frac{\Gamma(\gamma+1)}{\Gamma(\gamma-\alpha+1)} t^{\gamma-\alpha}, & \gamma \in N_0 \text{ and } \gamma \geq \lceil \alpha \rceil \text{ or } \gamma \notin N \text{ and } \gamma > \lfloor \alpha \rfloor, \end{cases} \tag{1.2}$$

$$(iv)\ D^\alpha \left(\sum_{i=1}^n c_i f_i(t) \right) = \sum_{i=1}^n c_i D^\alpha f_i(t), \quad \text{where} \ \ c_i \in R. \tag{1.3}$$

Definition 3. Suppose that $f(t), g(t) \in C[0, \eta]$ and $w(t)$ is a weight function, then

$$\| f(t) \|_w^2 = \int_0^\eta f^2(t) w(t) dt,$$

$$\langle f(t), g(t) \rangle_w = \int_0^\eta f(t) g(t) w(t) dt.$$

Theorem 1. (**Generalized Taylor's formula**) Suppose that $f(t) \in C[0, \eta]$ and $D^{k\alpha} f(t) \in C[0, \eta]$, where $k = 0, 1, ..., m$, $0 < \alpha \leq 1$ and $\eta > 0$. Then we have

$$f(t) = \sum_{i=0}^{m-1} \frac{t^{i\alpha}}{\Gamma(i\alpha+1)} D^{i\alpha} f(0^+) + \frac{t^{m\alpha}}{\Gamma(m\alpha+1)} D^{m\alpha} f(\xi), \tag{1.4}$$

with $0 < \xi \leq t$, $\forall t \in [0, \eta]$. And thus

$$|f(t) - \sum_{i=0}^{m-1} \frac{t^{i\alpha}}{\Gamma(i\alpha+1)} D^{i\alpha} f(0^+)| \leq M_\alpha \frac{t^{m\alpha}}{\Gamma(m\alpha+1)}, \tag{1.5}$$

where $M_\alpha \geq |D^{m\alpha} f(\xi)|$.

Proof: See Ref. [14].

The organization of the paper is expressed as follows: in section 2, the mathematical preliminaries to the problem is expressed. In section 3, the GFCFs and their properties are obtained.

In section 4, the work method is explained. Applications of the proposed method are shown in section 5. Finally, a brief conclusion is given in the last section.

2. MATHEMATICAL PRELIMINARIES

The integro-differential equation [15, 16]

$$\frac{d^2y}{dt^2} = g(t) - a(t)y(t) + b(t)\int_0^t \cos(w_p s)y(s)ds \tag{2.1}$$

where $a(t)$, $b(t)$ and $g(t)$ are given periodic functions of time may be easily found in the charged particle dynamics for some field configurations. Taking for instance the three mutually orthogonal magnetic field components $B_x = B_1\sin(w_p t)$, $B_y = 0, B_z = B_0$, the nonrelativistic equations of motion for a particle of mass m and charge q in this field configuration are

$$m\frac{d^2x}{dt^2} = q\left(B_0\frac{dy}{dt}\right), \tag{2.2}$$

$$m\frac{d^2y}{dt^2} = q\left(B_1\sin(w_p t)\frac{dz}{dt} - B_0\frac{dx}{dt}\right), \tag{2.3}$$

$$m\frac{d^2z}{dt^2} = q\left(-B_1\sin(w_p t)\frac{dy}{dt}\right). \tag{2.4}$$

By integration of (2.2) and (2.4) and replacement of the time first derivatives of z and x in (2.3) one has (2.1) with

$$a(t) = w_c^2 + w_f^2\sin^2(w_p t), \quad b(t) = w_f^2 w_p\sin(w_p t), \tag{2.5}$$

$$g(t) = w_f\sin(w_p t)z'(0) + w_c^2 y(0) + w_c x'(0), \tag{2.6}$$

where $w_c = qB_0/m$ and $w_f = qB_1/m$. Making the additional simplification that $x'(0) = 0$ and $y(0) = 0$, equation (2.1) is finally written as [16]

$$\frac{d^2y}{dt^2} = w_f\sin(w_p t)z'(0) - \left(w_c^2 + w_f^2\sin^2(w_p t)\right)y(t)$$

$$+ \left(w_f^2 w_p\sin(w_p t)\right)\int_0^t \cos(w_p s)y(s)ds \tag{2.7}$$

In this study, we consider the equation (2.1) with the following initial conditions

$$y(0) = \beta_0, \quad y'(0) = \beta_1 \tag{2.8}$$

There are methods to solve this equation, such as, He's Homotopy perturbation method [16], Chebyshev wavelet [17], Legendre multi-wavelets [18], Local polynomial regression [19], Shannon wavelets [20], Variational iteration method [21] and Homotopy analysis method [22].

In this paper, we attempt to introduce a new method based on the generalized fractional order Chebyshev orthogonal functions (GFCFs) of the first kind for solving the equation (2.1) with the initial conditions (2.8).

3. The Generalized Fractional Order Chebyshev Functions

In this section, first, the generalized fractional order of the Chebyshev functions (GFCF) have been defined, and then some properties and convergence of them for our method have been introduced.

3.1. **The Chebyshev functions.** The Chebyshev polynomials have been used in numerical analysis, frequently, including polynomial approximation, Gauss-quadrature integration, integral and differential equations and spectral methods. Chebyshev polynomials have many properties, for example orthogonal, recursive, simple real roots, complete in the space of polynomials. For these reasons, many researchers have employed these polynomials in their research [23, 24, 25, 26, 27, 28].

Using some transformations, the number of researchers extended Chebyshev polynomials to semi-infinite or infinite domains, for example by using $x = \frac{t-L}{t+L}, L > 0$ the rational functions introduced [29, 30, 31, 32, 33, 34].

In the proposed work, by transformation $z = 1-2(\frac{t}{\eta})^\alpha, \alpha > 0$ on the Chebyshev polynomials of the first kind, the fractional order of the Chebyshev orthogonal functions in the interval $[0, \eta]$ have been introduced, that they can use to solve these integro-differential equations.

3.2. **The GFCFs definition.** The efficient methods have been used by many researchers to solve the differential equations (DE) is based on the series expansion of the form $\sum_{i=0}^{n} c_i t^i$, such as Adomian decomposition method [35] and Homotopy perturbation method [36]. But the exact solution of many DEs can't be estimated by polynomial basis. Therefore, we have defined a new basis for Spectral methods to solve them as follows:

$$\Phi_n(t) = \sum_{i=0}^{n} c_i t^{i\alpha}.$$

Now by transformation $z = 1-2(\frac{t}{\eta})^\alpha, \alpha, \eta > 0$ on classical Chebyshev polynomials of the first kind, we defined the GFCFs in the interval $[0, \eta]$, that be denoted by ${}_\eta FT_n^\alpha(t) = T_n(1-2(\frac{t}{\eta})^\alpha)$. By this definition, the singular Sturm-Liouville differential equation of classical Chebyshev polynomials become:

$$\frac{\sqrt{\eta^\alpha - t^\alpha}}{t^{\frac{\alpha}{2}-1}} \frac{d}{dt} \left[\frac{\sqrt{\eta^\alpha - t^\alpha}}{t^{\frac{\alpha}{2}-1}} \frac{d}{dt} \, {}_\eta FT_n^\alpha(t) \right] + n^2\alpha^2 \, {}_\eta FT_n^\alpha(t) = 0, \quad t \in [0, \eta]. \qquad (3.1)$$

The ${}_\eta FT_n^\alpha(t)$ can be obtained using the recursive relation as follows ($n = 1, 2, \cdots$):

$${}_\eta FT_0^\alpha(t) = 1 \quad , \quad {}_\eta FT_1^\alpha(t) = 1 - 2(\tfrac{t}{\eta})^\alpha,$$

$${}_\eta FT_{n+1}^\alpha(t) = (2 - 4(\tfrac{t}{\eta})^\alpha) \, {}_\eta FT_n^\alpha(t) - \, {}_\eta FT_{n-1}^\alpha(t).$$

The analytical form of ${}_\eta FT_n^\alpha(t)$ of degree $n\alpha$ is given by

$${}_\eta FT_n^\alpha(t) \quad = \quad \sum_{k=0}^{n} (-1)^k \frac{n2^{2k}(n+k-1)!}{(n-k)!(2k)!} (\frac{t}{\eta})^{\alpha k}$$

$$= \sum_{k=0}^{n} \beta_{n,k,\eta,\alpha}.t^{\alpha k}, \ t \in [0, \eta], \tag{3.2}$$

where

$$\beta_{n,k,\eta,\alpha} = (-1)^k \frac{n 2^{2k}(n+k-1)!}{(n-k)!(2k)!\eta^{\alpha k}} \ and \ \beta_{0,k,\eta,\alpha} = 1.$$

Note that $_\eta FT_n^\alpha(0) = 1$ and $_\eta FT_n^\alpha(\eta) = (-1)^n$.

The GFCFs are orthogonal with respect to the weight function $w(t) = \frac{t^{\frac{\alpha}{2}-1}}{\sqrt{\eta^\alpha - t^\alpha}}$ in the interval $[0, \eta]$:

$$\int_0^\eta {}_\eta FT_n^\alpha(t) \ _\eta FT_m^\alpha(t) w(t) dt = \frac{\pi}{2\alpha} c_n \delta_{mn}. \tag{3.3}$$

where δ_{mn} is Kronecker delta, $c_0 = 2$, and $c_n = 1$ for $n \geq 1$. Eq. (3.3) is provable using properties of orthogonality in the Chebyshev polynomials.

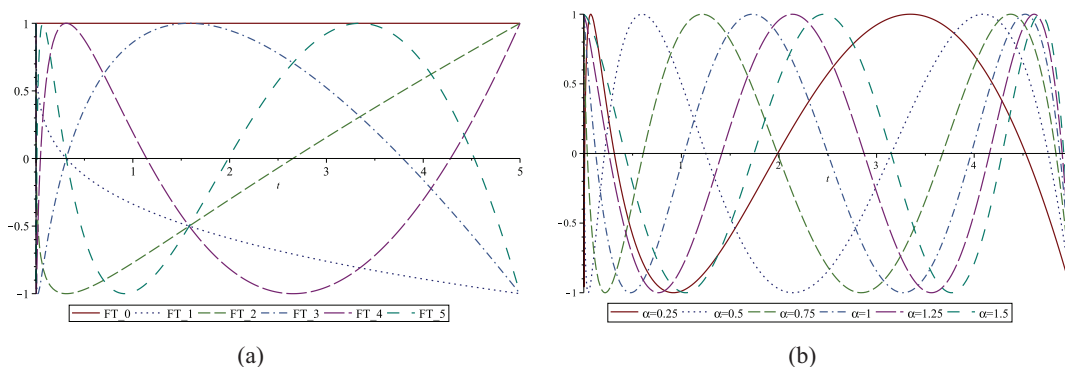Figs. 1 shown graphs of GFCFs for various values of n and α and $\eta = 5$.

FIGURE 1. (a) Graph of the GFCFs with $\alpha = 0.25$ and various values of n.
(b) Graph of the GFCFs with $n = 5$ and various values of α.

3.3. **Approximation of functions.** Any function $y(t) \in C[0, \eta]$ can be expanded as follows:

$$y(t) = \sum_{n=0}^{\infty} a_n \ _\eta FT_n^\alpha(t),$$

where the coefficients a_n obtain by inner product:

$$\langle y(t), \ _\eta FT_n^\alpha(t) \rangle_w = \langle \sum_{n=0}^{\infty} a_n \ _\eta FT_n^\alpha(t), \ _\eta FT_n^\alpha(t) \rangle_w$$

and using the property of orthogonality in the GFCFs:

$$a_n = \frac{2\alpha}{\pi c_n} \int_0^\eta {}_\eta FT_n^\alpha(t) y(t) w(t) dt, \ n = 0, 1, 2, \cdots.$$

In practice, we have to use first m-terms GFCFs and approximate $y(t)$:

$$y(t) \approx y_m(t) = \sum_{n=0}^{m-1} a_n \, {}_\eta FT_n^\alpha(t) = A^T \Phi(t), \tag{3.4}$$

with

$$A = [a_0, a_1, \cdots, a_{m-1}]^T, \tag{3.5}$$

$$\Phi(t) = [{}_\eta FT_0^\alpha(t), \, {}_\eta FT_1^\alpha(t), \cdots, \, {}_\eta FT_{m-1}^\alpha(t)]^T. \tag{3.6}$$

3.4. **Convergence of the method.** The following theorem shows that by increasing m, the approximation solution $f_m(t)$ is convergent to $f(t)$ exponentially.

Theorem 2. Suppose that $D^{k\alpha} f(t) \in C[0, \eta]$ for $k = 0, 1, ..., m$, and ${}_\eta F_m^\alpha$ is the subspace generated by $\{{}_\eta FT_0^\alpha(t), {}_\eta FT_1^\alpha(t), \cdots, {}_\eta FT_{m-1}^\alpha(t)\}$. If $f_m = A^T \Phi$ (in Eq. (3.4)) is the best approximation to $f(t)$ from ${}_\eta F_m^\alpha$, then the error bound is presented as follows

$$\| f(t) - f_m(t) \|_w \leq \frac{\eta^{m\alpha} M_\alpha}{2^m \Gamma(m\alpha + 1)} \sqrt{\frac{\pi}{\alpha.m!}},$$

where $M_\alpha \geq |D^{m\alpha} f(t)|$, $t \in [0, \eta]$.

Proof. By theorem 1, $y = \sum_{i=0}^{m-1} \frac{t^{i\alpha}}{\Gamma(i\alpha+1)} D^{i\alpha} f(0^+)$ and

$$|f(t) - y(t)| \leq M_\alpha \frac{t^{m\alpha}}{\Gamma(m\alpha + 1)},$$

since $A^T \Phi(t)$ is the best approximation to $f(t)$ in ${}_\eta F_m^\alpha$ and $y \in {}_\eta F_m^\alpha$, one has

$$\begin{aligned}
\| f(t) - f_m(t) \|_w^2 &\leq \| f(t) - y(t) \|_w^2 \\
&\leq \frac{M_\alpha^2}{\Gamma(m\alpha + 1)^2} \int_0^\eta \frac{t^{\frac{\alpha}{2}+2m\alpha-1}}{\sqrt{\eta^\alpha - t^\alpha}} dt \\
&= \frac{M_\alpha^2}{\Gamma(m\alpha + 1)^2} \frac{\eta^{2m\alpha} \pi}{\alpha 2^{2m} m!}.
\end{aligned}$$

Now by taking the square roots, the theorem can be proved. ∎

Theorem 3. The generalized fractional order of the Chebyshev function ${}_\eta FT_n^\alpha(t)$, has precisely n real zeros on interval $(0, \eta)$ in the form

$$t_k = \eta \left(\frac{1 - \cos(\frac{(2k-1)\pi}{2n})}{2} \right)^{\frac{1}{\alpha}}, \quad k = 1, 2, \cdots, n.$$

Moreover, $\frac{d}{dt} {}_\eta FT_n^\alpha(t)$ has precisely $n - 1$ real zeros on interval $(0, \eta)$ in the following points:

$$t_k' = \eta \left(\frac{1 - \cos(\frac{k\pi}{n})}{2} \right)^{\frac{1}{\alpha}}, \quad k = 1, 2, \cdots, n - 1.$$

Proof. The Chebyshev polynomial $T_n(x)$ has n real zeros [37, 38]:

$$x_k = \cos\left(\frac{(2k-1)\pi}{2n}\right), \ k = 1, 2, \cdots, n,$$

therefore $T_n(x)$ can be written as

$$T_n(x) = (x - x_1)(x - x_2) \cdots (x - x_n).$$

Using transformation $x = 1 - 2(\frac{t}{\eta})^\alpha$ yields to

$$FT_n^\alpha(t) = ((1 - 2(\frac{t}{\eta})^\alpha) - x_1)((1 - 2(\frac{t}{\eta})^\alpha) - x_2) \cdots ((1 - 2(\frac{t}{\eta})^\alpha) - x_n),$$

so, the real zeros of $_\eta FT_n^\alpha(t)$ are $t_k = \eta(\frac{1-x_k}{2})^{\frac{1}{\alpha}}$.
Also, the real zeros of $\frac{d}{dt}T_n(t)$ occurs in the following points [37]:

$$x'_k = \cos(\frac{k\pi}{n}), \ k = 1, 2, \cdots, n - 1.$$

Same as in previous, the absolute extremes of $_\eta FT_n^\alpha(t)$ are $t'_k = \eta(\frac{1-x'_k}{2})^{\frac{1}{\alpha}}$. $\blacksquare$

4. APPLICATION OF THE GFCF COLLOCATION METHOD

In this section, the GFCFs collocation method is applied to solve the integro-differential equation in the Eq. (2.1).
For satisfying the boundary conditions, the conditions in the Eq. (2.8) are satisfied as follows:

$$\widehat{y_m}(t) = \beta_0 + \beta_1 t + t^2 y_m(t), \tag{4.1}$$

where $y_m(t)$ is defined in the Eq. (3.4). Now, $\widehat{y_m}(t) = \beta_0$ and $\widehat{y_m}'(t) = \beta_1$ when t tends to zero, so the conditions in the Eq. (2.8) are satisfied.
To apply the collocation method, the residual function is constructed by substituting $\widehat{y_m}(t)$ in the Eq. (4.1) for $y(t)$ in the integro-differential equation (2.1):

$$Res(t) = \frac{d^2 y}{dt^2} - g(t) + a(t)y(t) - b(t) \int_0^t \cos(w_p s)y(s)ds. \tag{4.2}$$

The equations for obtaining the coefficient $\{a_i\}_{i=0}^{m-1}$ arise from equalizing $Res(t)$ to zero on m collocation points:

$$Res(t_i) = 0, \quad i = 0, 1, ..., m - 1. \tag{4.3}$$

In this study, the roots of the GFCFs in the interval $[0, \eta]$ (Theorem 3) are used as collocation points. By solving the obtained set of equations, we have the approximating function $\widehat{y_m}(t)$.
And also consider that all of the computations have been done by Maple 18 on a laptop with CPU Core i7, Windows 8.1 64bit, and 8GB of RAM.

5. ILLUSTRATIVE EXAMPLES

In this section, by using the present method, some well-known examples are solved to show efficiently and applicability GFCFs method based on Spectral method. The present method is applied to solve the integro-differential equation (2.1) and their outputs are compared with the corresponding analytical solution. These examples studied also by Dehghan [16], Khan [18] and Pathak [21], we will compare our results with their results to show the effectiveness of the present method.

Example 1. Consider the equation (2.1) with [16, 18, 21]

$$w_p = 2, \quad a(t) = \cos(t), \quad b(t) = \sin(t/2), \quad \beta_0 = 1, \quad \beta_1 = 0$$
$$g(t) = \cos(t) - t\sin(t) + \cos(t)\,(t\sin(t) + \cos(t))$$
$$- \sin(t/2)\left(\frac{2}{9}\sin(3t) - \frac{t}{6}\cos(3t) + \frac{t}{2}\cos(t)\right).$$

The exact solution of this equation is $y(t) = t\sin(t) + \cos(t)$. By applying the technique described in the last section, for satisfying the boundary conditions, the conditions are satisfied as $\widehat{y_m}(t) = 1 + t^2\, y_m(t)$. The residual function is constructed as follows:

$$Res(t) = \frac{d^2y}{dt^2} - g(t) + a(t)y(t) - b(t)\int_0^t \cos(w_p s)y(s)ds.$$

Therefore, to obtain the coefficient $\{a_i\}_{i=0}^{m-1}$; $Res(t)$ is equalized to zero at m collocation point. By solving this set of nonlinear algebraic equations, we can find the approximating function $\widehat{y_m}(t)$. Figure 2 shows the logarithmic graph of the absolute error and the residual error of the approximate solution and the analytic solution for $m = 20$ and $\alpha = 0.50$.
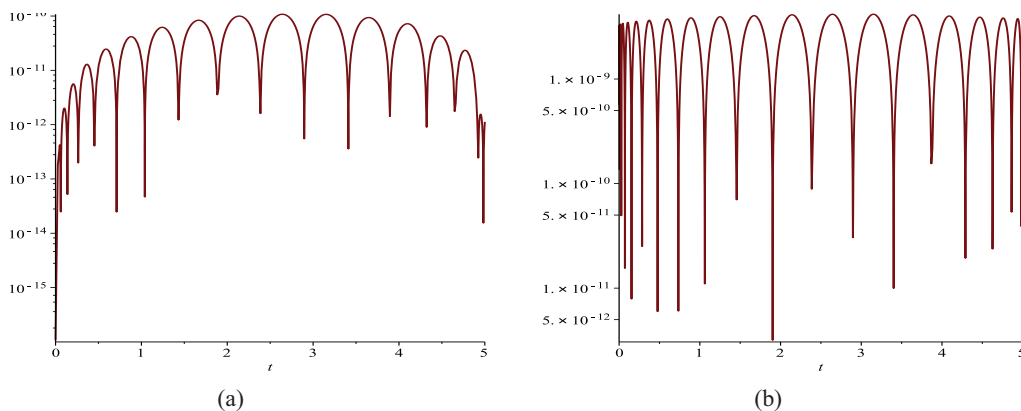

(a)   (b)

FIGURE 2. The logarithmic graphs of the absolute error and the residual error for example 1 with $m = 20$ and $\alpha = 0.50$. Graph of the (a) absolute, (b) residual error.

The resulting graph in comparison to the presented method and the exact solution is shown in Figure 3(a). In Figure 3(b) to show the convergence of the present method, we showed that by increasing the m the residual function decreases, where $\alpha = 0.50$.
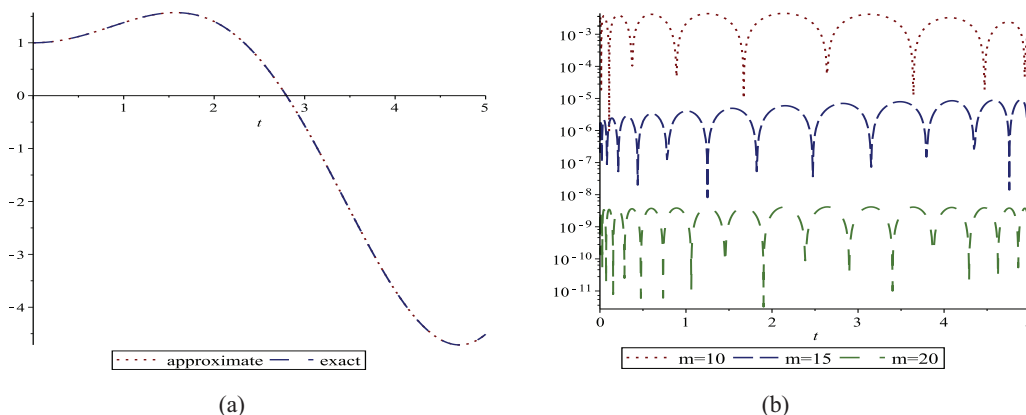

(a)   (b)

FIGURE 3. (a) Obtained graph in comparison to the exact solution with $m = 20$ and $\alpha = 0.50$. (b) Residual functions for $m = 10,\ 15,\ 20$ and $\alpha = 0.50$, to show the convergence rate of the GFCF method for example 1.

Table 1 compares the error norm $\|y - y_m\|_2$ by the present method and Dehghan [16] for examples 1-3.

TABLE 1. Comparison of error norm $\|y - y_m\|_2$ by Dehghan [16] and the present method for examples 1-3

Example	Dehghan [16]	Present method
Example 1	6.826965141905116e-13	1.4691408679507079e-20
Example 2	2.440936203513114e-13	8.8876680000000000e-39
Example 3	3.279510650660257e-12	2.6061709227703975e-95

Table 2 compares the obtained values of $y(t)$ by the present method and the values given by Khan [18] (Legendre multi-wavelets) and Pathak [21] (Variational iteration method), it shows that the results obtained in the present method are more accurate.

TABLE 2. Obtained values of $y(t)$ for example 1 by Khan, Pathak, and the present method with $m = 20$.

t	Khan [18]	Pathak [21]	Present method	Exact Solution	Abs. Err.	Res. Err.
0.1	1.006711649	1.004987505	1.004987506944	1.004987506942	1.997e-12	3.329e-9
0.2	1.019729643	1.019800356	1.019800443994	1.019800444000	5.546e-12	3.391e-9
0.3	1.043967189	1.043991584	1.043992551130	1.043992551124	6.216e-12	1.032e-9
0.4	1.078484444	1.076823090	1.076828330937	1.076828330926	1.072e-11	3.318e-9
0.5	1.116769872	1.117276231	1.117295331180	1.117295331192	1.182e-11	1.190e-9
0.6	1.164117090	1.164067124	1.164121098922	1.164121098946	2.436e-11	3.746e-9
0.7	1.216007719	1.215666930	1.215794568347	1.215794568350	3.654e-12	1.388e-9
0.8	1.270604841	1.270327190	1.270591582096	1.270591582066	2.975e-11	2.415e-9
0.9	1.326616801	1.326109990	1.326604186976	1.326604186935	4.096e-11	3.827e-9

Example 2. Consider the equation (2.1) with [16, 18, 21]

$$w_p = 1, \quad a(t) = -\sin(t), \quad b(t) = \sin(t), \quad \beta_0 = 1, \quad \beta_1 = 2/3$$

$$g(t) = \frac{1}{9}e^{-\frac{t}{3}} - \sin(t)\left(e^{-\frac{t}{3}} + t\right)$$

$$- \sin(t)\left(-\frac{3}{10}\cos(t)e^{-\frac{t}{3}} + \frac{9}{10}\sin(t)e^{-\frac{t}{3}} + \cos(t) + t\sin(t) - \frac{7}{10}\right).$$

The exact solution of this equation is $y(t) = e^{-\frac{t}{3}} + t$. By applying the technique described in the last section, the conditions are satisfied as : $\widehat{y_m}(t) = 1 + \frac{2}{3}t + t^2 y_m(t)$, and construct the residual functions as follows:

$$Res(t) = \frac{d^2y}{dt^2} - g(t) + a(t)y(t) - b(t)\int_0^t \cos(w_p s)y(s)ds.$$

Figure 4 shows the logarithmic graph of the absolute error and the residual error of the approximate solution and the exact solution for $m = 20$ and $\alpha = 0.50$.
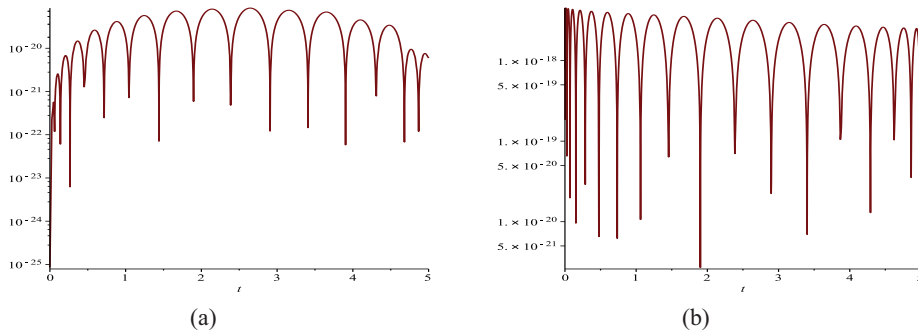

(a) (b)

FIGURE 4. The logarithmic graphs of the (a) absolute error and the (b) residual error for example 2 with $m = 20$ and $\alpha = 0.50$.

The resulting graph in comparison to the present method and the exact solution is shown in Figure 5 (a). To show the convergence of the present method to solve this example with $\alpha = 0.50$ in Figure 5 (b), we showed that by increasing the m the residual function decreases.
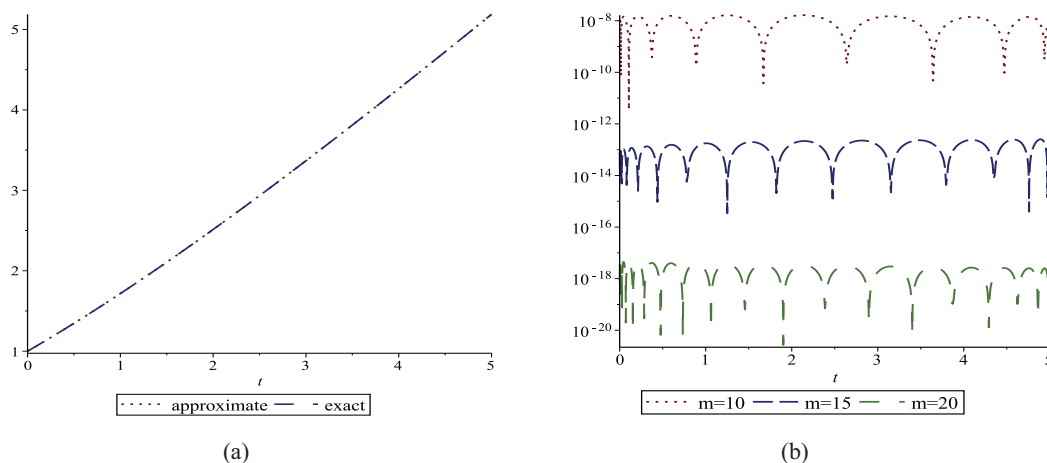

(a)

(b)

FIGURE 5. (a) Obtained graph in comparison with the exact solution with $m = 20$ and $\alpha = 0.50$. (b) Residual functions for $m = 10, 15, 20$ and $\alpha = 0.50$, to show the convergence rate of GFCF method for example 2.

Table 1 compares the error norm $\|y - y_m\|_2$ by the present method and Dehghan [16] for examples 1-3. Table 3 compares the obtained values of $y(t)$ by the present method and the values given by Khan [18] (Legendre multi-wavelets) and Pathak [21] (Variational iteration method), it shows that the results obtained in the present method are more accurate.

TABLE 3. Obtained values of $y(t)$ for example 2 by Khan (Legendre multi-wavelets), Pathak (Variational iteration method), and the present method with $m = 20$

t	Khan [18]	Abs. Err. Pathak [21]	Present method	Exact Solution	Abs. Err.	Res. Err.
0.1	1.067409867	5.0900e-13	1.06721610048200590204	1.06721610048200590204	2.5e-21	4.1e-18
0.2	1.135498873	1.3237e-10	1.13550698503161773772	1.13550698503161773773	6.6e-21	4.0e-18
0.3	1.204831254	3.4433e-09	1.20483741803595957317	1.20483741803595957316	6.8e-21	1.1e-18
0.4	1.275363888	3.4759e-08	1.27517331904294745400	1.27517331904294745399	1.2e-20	3.7e-18
0.5	1.346379637	2.0843e-07	1.34648172489061407403	1.34648172489061407404	1.2e-20	1.2e-18
0.6	1.418729558	————	1.41873075307798185864	1.41873075307798185866	2.6e-20	3.9e-18
0.7	1.491932333	————	1.49188956633678166437	1.49188956633678166437	5.1e-21	1.4e-18
0.8	1.565927886	————	1.56592833836464869274	1.56592833836464869271	2.8e-20	2.4e-18
0.9	1.640830867	————	1.64081822068171786610	1.64081822068171786606	4.1e-20	3.8e-18

Example 3. Consider equation (2.1) with [16, 18, 21]

$$w_p = 3, \quad a(t) = 1, \quad b(t) = \sin(t) + \cos(t), \beta_0 = 2, \quad \beta_1 = -5,$$

$$g(t) = -t^3 + t^2 - 11t + 4 - (\sin(t) + \cos(t))$$

$$(-\frac{t^3}{3}\sin(3t) - \frac{t^2}{3}\cos(3t) - \frac{13}{27}\cos(3t) - \frac{13}{9}t\sin(3t)$$

$$+\frac{t^2}{3}\sin(3t) + \frac{16}{27}\sin(3t) + \frac{2t}{9}\cos(3t) + \frac{13}{27}),$$

The exact solution of this equation is $y(t) = -t^3 + t^2 - 5t + 2$. By applying the technique described in the last section, the conditions are satisfied as : $\widehat{y_m}(t) = 2 - 5t + t^2\,y_m(t)$. The residual function is constructed as follows :

$$Res(t) = \frac{d^2y}{dt^2} - g(t) + a(t)y(t) - b(t)\int_0^t \cos(w_p s)y(s)ds.$$

Figure 6 shows the logarithmic graph of the absolute error and the residual error of the approximate solution and the exact solution for $m = 5$ and $\alpha = 0.50$.
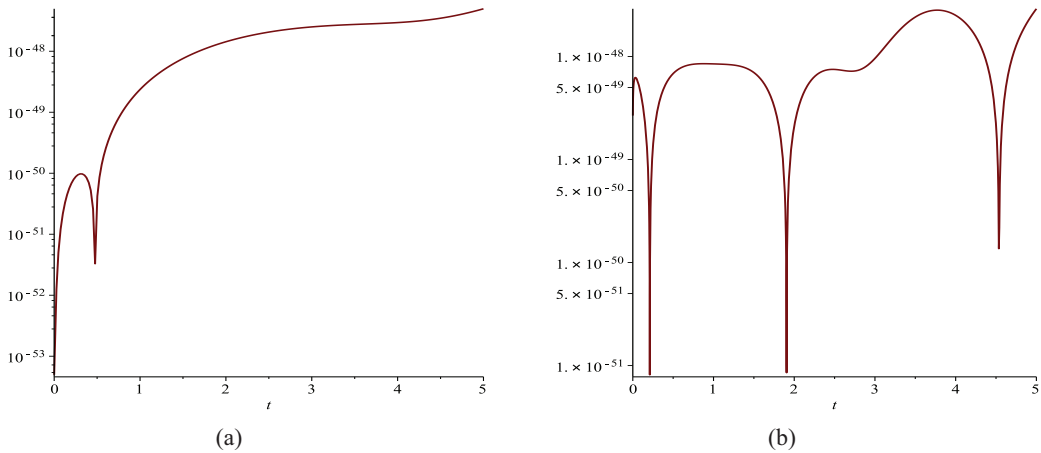

(a)   (b)

FIGURE 6. The logarithmic graphs of the (a) absolute error and the (b) residual error for example 2 with $m = 5$ and $\alpha = 0.50$.

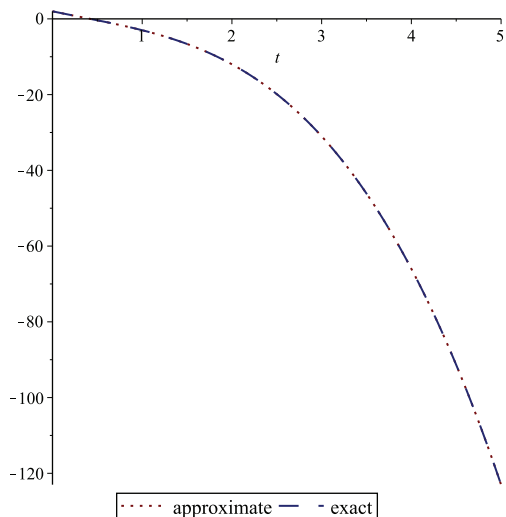The resulting graph in comparison to the present method and the exact solutions is shown in Figure 7.

FIGURE 7. Obtained graph in comparison to the exact solution for example 3 with $m = 5$ and $\alpha = 0.50$.

Table 1 compares the error norm $\|y - y_m\|_2$ by the present method and Dehghan [16] for examples 1-3. Table 4 compares the obtained values of $y(t)$ by the present method and the values given by Khan [18] (Legendre multi-wavelets) and Pathak [21] (Variational iteration method), it shows that the results obtained in the present method are more accurate.

TABLE 4. Obtained values of $y(t)$ for example 3 by Khan, Pathak, and the present method with $m = 5$.

t	Khan [18]	Abs. Err. Pathak [21]	Present method	Exact Solution	Abs. Err.	Res. Err.
0.1	1.510232801	—————	1.50900000	1.509	0	4.331e-49
0.2	1.031768407	0.0000e-00	1.03200000	1.032	0	3.845e-50
0.3	0.563149603	—————	0.56300000	0.563	0	2.869e-49
0.4	0.096626905	1.5399e-12	0.09600000	0.096	0	5.244e-49
0.5	-0.373166748	—————	-0.37500000	-0.375	0	6.837e-49
0.6	-0.856012437	4.1554e-11	-0.85600000	-0.856	0	7.799e-49
0.7	-1.353869376	—————	-1.35300000	-1.353	0	8.296e-49
0.8	-1.871984718	2.1376e-10	-1.87200000	-1.872	0	8.489e-49
0.9	-2.419488059	—————	-2.41900000	-2.419	0	8.517e-49

6. Conclusion

The main goal of this paper was to introduce a new orthogonal basis, namely the generalized fractional order of the Chebyshev orthogonal functions (GFCF) to construct an approximation to the solution of the integro-differential equation arising in oscillating magnetic fields. The presented results show that the introduced basis for the collocation spectral method is efficient and applicable. Our results have better accuracy with lesser m, and the absolute error as compared to the exact solution. A comparison was made of the exact solution and the present method. As shown, the method is converging and has an approximate accuracy and stability, and the error decreases with increasing m.

Acknowledgements

References

[1] J.P. Boyd, **Chebyshev spectral methods and the Lane-Emden problem**, Numer. Math. Theor. Meth. Appl., **4**(2) (2011) 142–157.

[2] K. Parand, M. Nikarya, J.A. Rad, **Solving non-linear Lane-Emden type equations using Bessel orthogonal functions collocation method**, Celest. Mech. Dyn. Astr., **16**(21) (2013) 97–107.

[3] J. Shen, T. Tang, L.L. Wang, **Spectral Methods Algorithms, Analysis and Applications**, 1st edition, Springer, New York (2001).

[4] J.A. Rad, K. Parand, L.V. Ballestra, **Pricing European and American options by radial basis point interpolation**, Appl. Math. Comput., **251** (2015) 363–377.

[5] L. D'Amore, **Remarks on numerical algorithms for computing the inverse Laplace transform**, Ricerche mat., **63**(2) (2014) 239–252.

[6] K. Parand, M. Dehghan, A. Pirkhedri, **The Sinc-collocation method for solving the Thomas-Fermi equation**, J. Comput. Appl. Math., **237**(1) (2013) 244–252.

[7] J. Shen, T. Tang, **High Order Numerical Methods and Algorithms**. Chinese Science Press, Chinese (2005).

[8] J.A. Rad, K. Parand, S. Kazem, **A Numerical Investigation to Viscous Flow Over Nonlinearly Stretching Sheet with Chemical Reaction, Heat Transfer and Magnetic Field**, Int. J. Appl. Comput. Math., doi:10.1007/s40819-016-0143-1, (2016) 1–17.

[9] J.A. Rad, K. Parand, S. Abbasbandy, **Local weak form meshless techniques based on the radial point interpolation (RPI) method and local boundary integral equation (LBIE) method to evaluate European and American options**, Commun. Nonlinear Sci. Num. Simul., **22**(1) (2015) 1178–1200.

[10] K. Parand, M. Dehghan, A. Taghavi, **Modified generalized Laguerre function Tau method for solving laminar viscous flow: The Blasius equation**, Int. J. Numer. Method. H., **20**(7) (2010) 728–743.

[11] S. Kazem, S. Abbasbandy, S. Kumar, **Fractional-order Legendre functions for solving fractional-order differential equations**, Appl. Math. Modell., **37**(2013) 5498–5510

[12] A.A. Kilbas, H.M. Srivastava, J.J. Trujillo, **Theory and Applications of Fractional Differential Equations**, Elsevier, San Diego, 2006.

[13] M. Delkhosh, **Introduction of Derivatives and Integrals of Fractional order and Its Applications**, Appl. Math. Phys., **1**(4) (2013) 103–119.

[14] Z. Odibat, S. Momani, **An algorithm for the numerical solution of differential equations of fractional order**, J. Appl. Math. Inform. **26** (2008) 15–27.

[15] J.M. Machado, M.Tsuchida, **Solutions for a class of integro-differential equations with time periodic coefficients**, Appl. Math. E-Notes, **2** (2002) 66–71.

[16] M. Dehghan, F. Shakeri, **Solution of an Integro-Differential Equation Arising in Oscillating Magnetic Fields Using He's Homotopy Perturbation Method**, Prog. Electromag. Res., **78** (2008) 361–376.

[17] M. Ghasemi, **Numerical technique for integro-differential equations arising in oscillating magnetic fields**, Iranian J. Sci. Tech., **38**A4 (2014) 473–479.

[18] Y. Khan, M. Ghasemi, S. Vahdati, M. Fardi, **Legendre Multi-Wavelets to Solve oscillating magnetic fields integro-differential equations**, U.P.B. Sci. Bull. Ser. A, **76**(1) (2014) 51–58.

[19] F. Li, T. Yan, L. Su, **Solution of an Integral-Differential Equation Arising in Oscillating Magnetic Fields Using Local Polynomial Regression**, Adv. Mech. Eng., (2014) 9 pages.

[20] K. Maleknejad, M. Hadizadeh, M. Attary, **On The Approximate Solution of Integro-Differential Equation Arising in Oscillating Magnetic Fields**, App. Math., **58**(5) (2013) 595–607.

[21] M.R Pathak, P. Joshi, **High Order Numerical Solutionof a Volterra Integro-Differential Equation Arising in Oscillating Magnetic Fields using Variational Iteration Method**, Int. J. Adv. Sci. Tech., **69** (2014) 47–56.

[22] H. Saberi-Nik, S. Effati, R. Buzhabadi, **Analytic approximate solution for an integro-differential equation arising in oscillating magnetic fields using homotopy analysis method**, Iranian J. Optim., **3** (2010) 518–535.

[23] M.R. Eslahchi, M. Dehghan, S. Amani, **Chebyshev polynomials and best approximation of some classes of functions**, J. Numerical Math., **23** (1) (2015) 41–50.

[24] K. Parand, M. Delkhosh, **Solving Volterra's population growth model of arbitrary order using the generalized fractional order of the Chebyshev functions**, Ricerche Mat., **65** (2016) 307–328.

[25] E. H. Doha, A.H. Bhrawy, S. S. Ezz-Eldien , **A Chebyshev spectral method based on operational matrix for initial and boundary value problems of fractional order**, Comput. Math. Appl., **62** (2011) 2364–2373.

[26] A. Nkwanta and E.R. Barnes, **Two Catalan-type Riordan arrays and their connections to the Chebyshev polynomials of the first kind**, J. Integer Seq., **15** (2012) 1–19.

[27] A.H. Bhrawy, A.S. Alofi, **The operational matrix of fractional integration for shifted Chebyshev polynomials**, Appl. Math. Lett., **26** (2013) 25–31.

[28] A. Saadatmandi, M. Dehghan, **Numerical solution of hyperbolic telegraph equation using the Chebyshev tau method**, Numer. Meth. Part. D. E., **26** (1) (2010) 239–252.

[29] K. Parand, A. Taghavi, M. Shahini, **Comparison between rational Chebyshev and modified generalized Laguerre functions pseudospectral methods for solving Lane-Emden and unsteady gas equations**, Acta Phys. Pol. B, **40**(12) (2009) 1749–1763.

[30] K. Parand, M. Shahini, A. Taghavi, **Generalized Laguerre polynomials and rational Chebyshev collocation method for solving unsteady gas equation**, Int. J. Contemp. Math. Sci., **4**(21) (2009) 1005–1011.

[31] K. Parand, S. Abbasbandy, S. Kazem, A.R. Rezaei, **An improved numerical method for a class of astrophysics problems based on radial basis functions**, Phy. Scripta, **83** (2011) 015011, 11 pages.

[32] K. Parand, M. Shahini, **Rational Chebyshev pseudospectral approach for solving Thomas-Fermi equation**, Phys. Lett. A, **373** (2009) 210–213.

[33] K. Parand, S. Khaleqi, **The Rational Chebyshev of Second Kind Collocation Method for Solving a Class of Astrophysics Problems**, Euro. Phys. J. Plus, **131** (2016) 1–24.

[34] K. Parand, M. Shahini, M. Dehghan, **Solution of a laminar boundary layer flow via a numerical method**, Commun. Nonlinear Sci. Num. Simul., **15**(2) (2010) 360–367.

[35] G. Adomian, **Solving Frontier problems of Physics: The decomposition method**, Kluwer Academic Publishers, 1994.

[36] S.J. Liao, **The proposed homotopy analysis technique for the solution of nonlinear problems**, PhD thesis, Shanghai Jiao Tong University, 1992.

[37] M.S.H. Chowdhury, I. Hashim, **Solution of a class of singular second-order IVPs by Homotopy-Perturbation method**, Phys. Lett. A, **365** (2007) 439–447.

[38] M.A. Darani, M. Nasiri, **A fractional type of the Chebyshev polynomials for approximation of solution of linear fractional differential equations**, Comp. Meth. Diff. Equ., **1** (2013) 96–107.